ResearchGate

See discussions, stats, and author profiles for this publication at: https://www.researchgate.net/publication/30498066

Experimental and Theoretical Evaluation of the Reactions Leading to Formation of Internal Double Bonds in Suspension PVC

ARTICLE *in* MACROMOLECULES · JUNE 2008

Impact Factor: 5.8 · DOI: 10.1021/ma800583k · Source: OAI

CITATIONS
22

READS
33

7 AUTHORS, INCLUDING:

Jindra Purmova
AkzoNobel
8 PUBLICATIONS **149** CITATIONS

SEE PROFILE

Michelle L Coote
Australian National University
214 PUBLICATIONS **5,687** CITATIONS

SEE PROFILE

Available from: Michelle L Coote
Retrieved on: 26 January 2016

Experimental and Theoretical Evaluation of the Reactions Leading to Formation of Internal Double Bonds in Suspension PVC

Jindra Purmová,[†,‡] Kim F. D. Pauwels,[†] Michela Agostini,[†] Maarten Bruinsma,[†] Eltjo J. Vorenkamp,[†] Arend J. Schouten,*[,†] and Michelle L. Coote*[,§]

Zernike Institute of Advanced Materials, Department of Polymer Science, University of Groningen, Nijenborgh 4, 9747 AG Groningen, The Netherlands; ARC Centre for Free Radical Chemistry and Biotechnology, Research School of Chemistry, Australian National University, Canberra ACT 0200, Australia

Received March 17, 2008; Revised Manuscript Received April 29, 2008

ABSTRACT: The number of internal double bonds in poly(vinyl chloride) (PVC) samples was studied as a function of molecular weight at various monomer conversions. These defect structures were found to exhibit end-group-like characteristics: their concentration per chain was largely constant as a function of molecular weight. This tendency was independent of the degree of conversion. An intramolecular mechanism for formation of unsaturated structures and their location between carbons 5−6 were confirmed via ^{13}C NMR studies. High-level ab initio calculations showed that a 1−6 hydrogen transfer reaction was the most likely origin for these structures, though a second mechanism involving backbiting of the 1−2 Cl shifted head-to-head radical followed by β-chlorine elimination and then transfer to monomer could also contribute at lower conversions. From the experimental analysis and theoretical calculations, it emerged that this backbiting reaction is stereoselective, with the isotactic conformation appearing to be more resistant. However, from the ab initio calculations and earlier results of other research groups it also seems likely that hydrogen abstraction from chloroallylic end groups and further propagation of such radical is a concurrent route to internal double bonds. The evidence collected in this paper point to hydrogen abstraction reactions, especially backbiting and abstraction from chloroallylic end groups, as reactions for which inhibition should have a beneficial effect on the thermal stability of PVC.

Introduction

The thermal and photochemical stability of poly(vinyl chloride) (PVC) is much lower than expected from its chemical structure. This is due to the presence of structural defects containing tertiary or allylic chloride, which are formed by chain transfer reactions during the free-radical polymerization process.[1−6] The degradation of PVC, which starts from these labile points, consists of elimination of hydrogen chloride leading to formation of polyenes, rendering a brittle red-brown material with poor mechanical properties. PVC products are nonetheless employed in many important applications, and this is made possible by the inclusion of stabilizers—containing heavy metals—during the processing of PVC to its products.[7] Due to their negative impact on the environment, these stabilizers are currently being phased out under a voluntary agreement signed by the European PVC manufacturers.[8] Unfortunately, environmentally more friendly alternatives (such as zinc carboxylates or polyols) are less effective and can affect, for example, the early color of the material.[7] It would thus be desirable if the formation of the structural defects themselves could be minimized, thereby improving the *inherent* stability of the PVC.

Allylic chlorides are defects associated with internal unsaturations within the polymer backbone. On the basis of dehydrochlorination measurements under argon flow, allylic chlorides have been shown to be less reactive than tertiary chlorides, but they are more susceptible to the presence of HCl.[9] The side-reactions that are reported in the literature to give rise to internal unsaturations are intra- or intermolecular hydrogen abstraction from the methylene unit by the growing polymer chains, and subsequent β-elimination of a chlorine radical by transfer to monomer.[5,10] Another proposed route involves the in situ conversion of chloroallylic end groups to internal unsaturations via hydrogen abstraction followed by further propagation.[10] However, the relative importance of these processes has not as yet been revealed.

In the present work, we examine the molecular weight dependence of the internal double bonds in PVC. According to earlier studies, the unsaturated defect structures are mostly contained in the low molecular weight fractions of the polymer.[4,11] Understanding this molecular weight dependence, and its relationship to other process conditions such as conversion, can help to provide an insight into the mechanism of formation of these defects. In what follows, we measure the concentration of internal unsaturations as a function of chain length in PVC samples formed at various monomer conversions. To assist in the mechanistic interpretation of the results, we also use high-level ab initio molecular orbital calculations to estimate the rate coefficients for the various possible intramolecular hydrogen transfer reactions in vinyl chloride polymerization and other possible side reactions.

Experimental Section

Polymerization. Vinyl chloride monomer (VCM, 99.97%, Shin Etsu PVC BV, The Netherlands) was polymerized by radical suspension polymerization at 57 °C in a 1-L steel autoclave by a method described elsewhere.[12]

Fractionation. Fractionation of PVC samples was performed via a modified fractional precipitation method.[13,14] The lowest molecular weight fractions, which could not be obtained by fractionation, were isolated by stirring the PVC powder overnight in a mixture of hexane and acetone (75:25). The material insoluble in this mixture of solvents was removed via filtration. The remaining liquid was then evaporated in a rotary evaporator, leaving the low

* Corresponding author. E-mail: (M.L.C.) mcoote@rsc.anu.edu.au; (A.J.S.) A.J.Schouten@rug.nl.
[†] Zernike Institute of Advanced Materials, Department of Polymer Science, University of Groningen.
[‡] Present address, Dept. CAP-CWA, Research & Technology Center, Akzo Nobel Chemicals, Velperweg 76, 6824 BM Arnhem, The Netherlands.
[§] ARC Centre for Free Radical Chemistry and Biotechnology, Research School of Chemistry, Australian National University.

10.1021/ma800583k CCC: $40.75 © 2008 American Chemical Society
Published on Web 07/12/2008

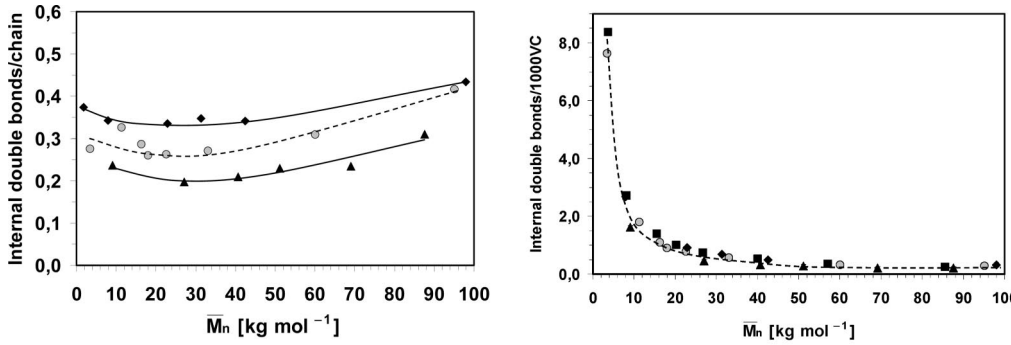

Figure 1. Dependence of the number of internal double bonds (a) per chain and (b) per 1000 VC on $\bar{M}_n$ for fractions of suspension PVC samples of different monomer conversions polymerized at 57.5 °C. Key: (▲) 23.7%; (gray circle) 87.2%; (♦) 96.4%.

Scheme 1. Intramolecular Hydrogen Transfer Reactions Possibly Occurring During the Propagation of Radical VC Polymerization

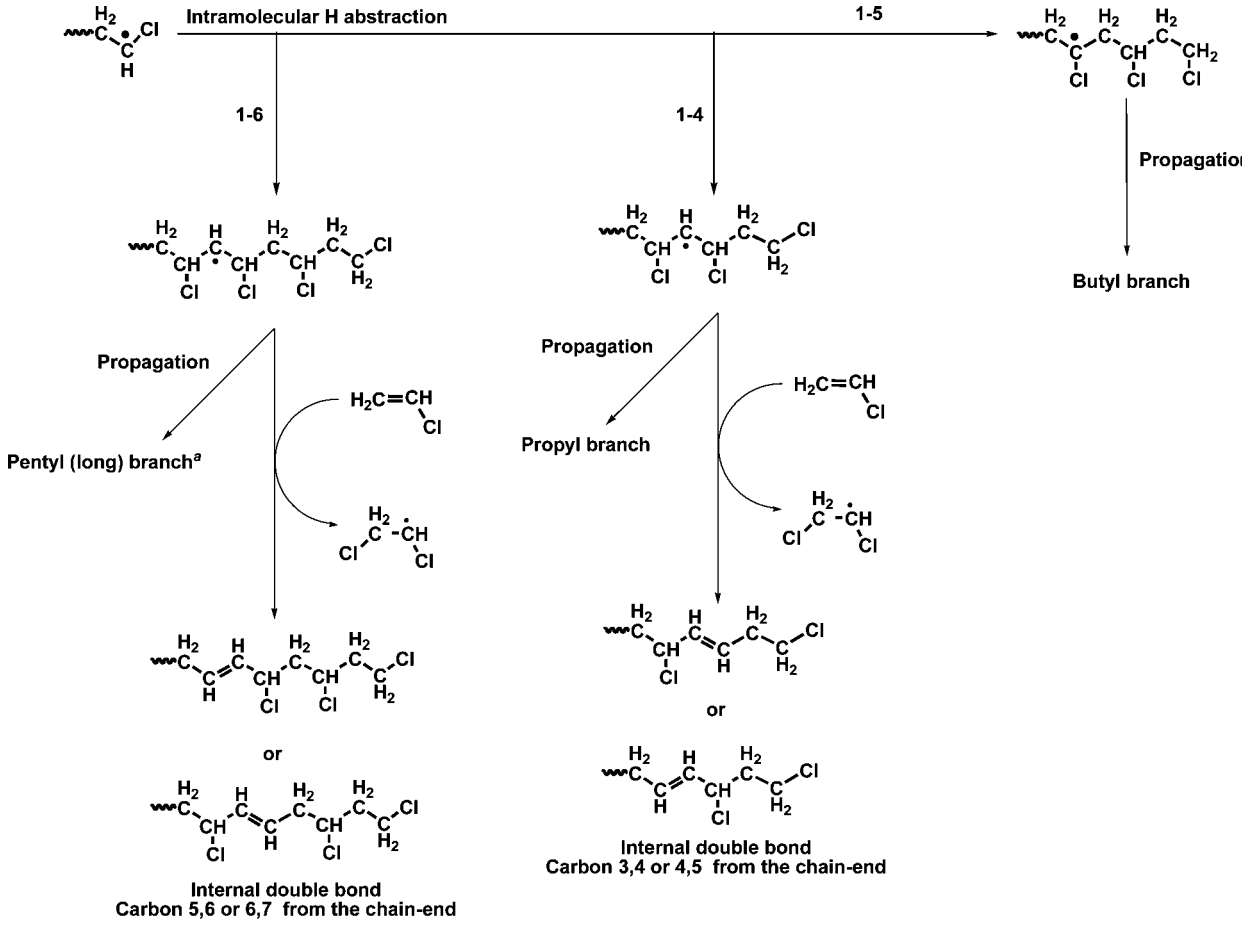

[a] Further propagation of the radical formed by 1−6 backbiting would give rise to a pentyl branch. According to Hjertberg et al.,[3] only branches up to 5 carbons can be distinguished using ^{13}C spectra of reductively dehalogenated PVC. This structure would give the same peaks as long branches formed by intermolecular transfer.

molecular weight PVC, which was then dried at room temperature under vacuum. The resulting fractions were characterized by GPC and ^1H and ^{13}C (performed on reductively dehalogenated material) NMR spectroscopy using the same procedure described in detail in refs 12 and 14. The tacticity was determined by analysis of ^{13}C spectra of the unmodified resin.

Reductive Dehalogenation. Reductive dehalogenation was carried out using a modified[12] one-step variant[15] of the method developed by Starnes et al.[16]

Computational Procedures. Standard ab initio molecular orbital theory and density functional theory calculations were carried out using GAUSSIAN 03[17] and MOLPRO 2000.6.[18] Calculations were performed at a high level of theory, G3(MP2)-RAD//MPW1K/6−31+G(d,p), which was chosen on the basis of a previous assessment study.[19] The gas-phase rate coefficients for the propagation and transfer reactions were calculated at 57.5 °C via standard transition state theory, in conjunction with the harmonic oscillator approximation. The hydrogen abstraction rate coefficients also incorporate Eckart tunneling corrections.[20] Full details of these calculations are provided in an earlier publication.[12,21]

Results and Discussion

The presence of internal double bonds in PVC was studied as a function of molecular weight for three PVC specimens,

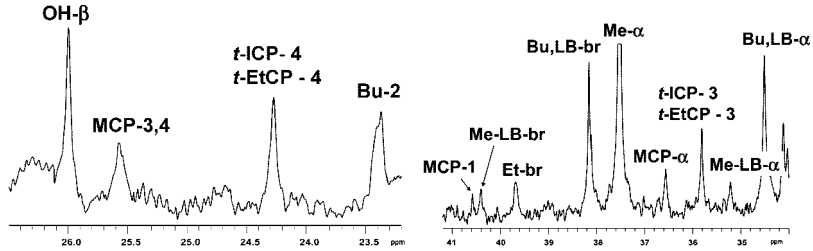

Figure 2. Expansions of the ^{13}C spectrum of the dehalogenated low molecular extract of suspension PVC at 87.2% conversion prepared at 57.5 °C. Signals of monoalkylcyclopentane (MCP), *trans*-ethylcyclopentane (*t*EtCP) and *trans*-internal cyclopentane (*t*ICP) moieties are shown (For the numbering of the C atoms of the cyclopentane structures, see Scheme 2). OH-β is the carbon in position β to the OH groups in the $-CH_2CH_2CH(OH)CH_2CH_2-$ segments, probably originating from air oxidation during the reductive dehalogenation.

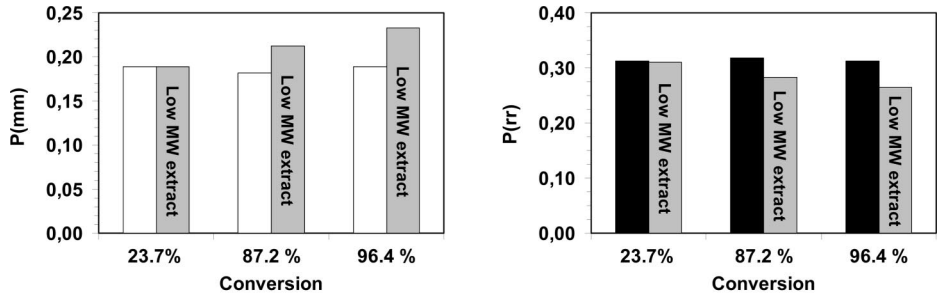

Figure 3. Comparison of the content of (a) isotactic (mm) and (b) syndiotactic (rr) triads in nonfractionated PVC of different monomer conversion, and in the corresponding low molecular weight extracts. White and black columns represent nonfractionated PVC, whilst gray columns represent low molecular weight extracts. PVC samples were polymerized by suspension polymerization at 57.5 °C and the low molecular weight part was obtained by extraction with the mixture of hexane and acetone (75:25) as described in the Experimental Section.

Scheme 2. Cyclopentane Structures Derived from Reductive Cyclizations of Unsaturated Structures Located at Different Positions Relative to the Chain End

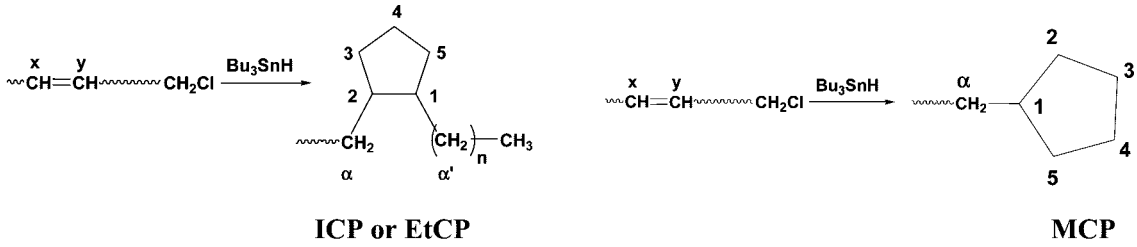

Position of the expected double bond	Expected cyclopentane structure
x=3, y=2, n=1	Ethyl cyclopentane (EtCP)
x=4, y=3	None
x=5, y=4, n=3	Butyl cyclopentane
x=7, y=6, n=5	Hexyl cyclopentane
x=6, y=5	Monoalkyl cyclopentane (MCP)
x,y =randomly in the chain	Internal cyclopentane (ICP)

isolated at 23.7%, 87.2%, and 96.4% conversion. Each of the PVC samples was fractionated, with the fractions (and the low molecular weight extracts) uniformly covering the molecular weight range. The molecular weight data for all of the samples are provided in Table S1 (Supporting Information). In general, the fractions had narrower molecular weight distributions than the original polymer, and the number ($\bar{M}_n$) and weight ($\bar{M}_w$) average molecular weight decreased for each fraction. Fractions of each sample were then studied by ^1H NMR, in order to measure the concentration of the internal unsaturations. The dependence of the numbers of these types of defects on molecular weight and conversion, and its consequences for the mechanism of their formation, will now be discussed in turn.

Effect of Chain Length and Conversion. Figure 1 a shows the concentration of internal unsaturations *per chain* as a function of chain length for each of the PVC specimens. In general terms, the concentration per chain is relatively insensitive to chain length, increasing by only 0.1 over the entire molecular weight range. The confidence intervals were 0.03 for both the

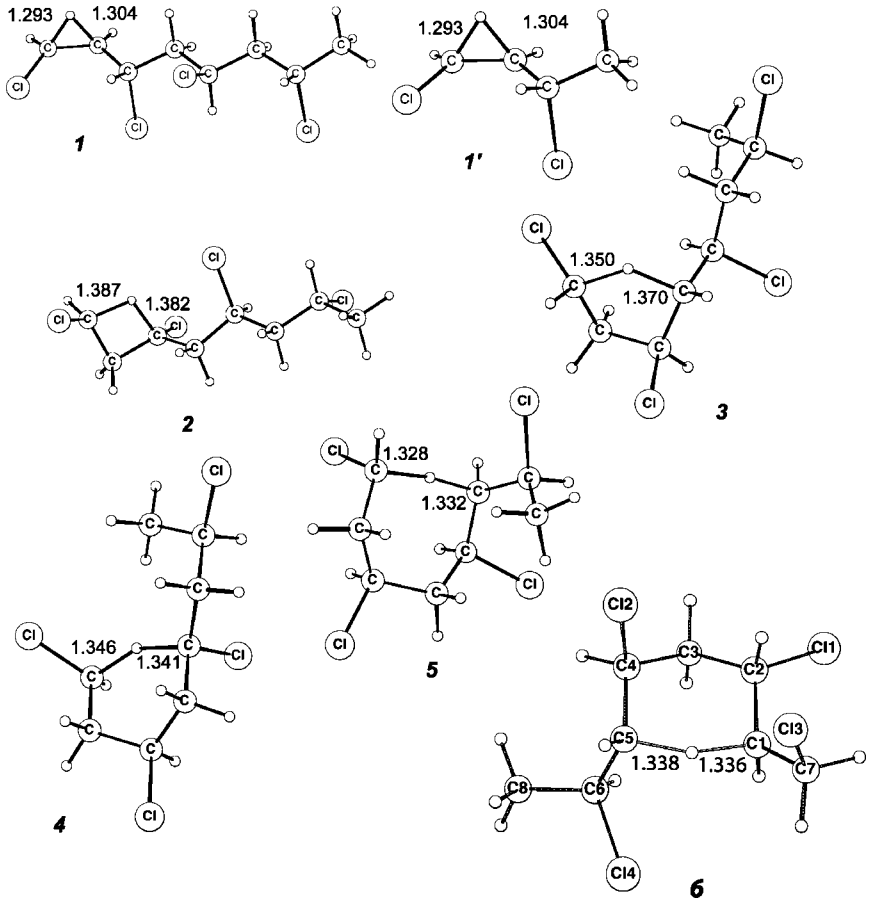

Figure 4. MPW1K/6−31+G(d,p) optimized geometries of the transition structures for the intramolecular hydrogen transfer reactions in Scheme 3.

23.7% and 96.4% conversion data sets and 0.04 for the 87.2% conversion data set.

Expressed as a concentration per 1000 VC, the internal unsaturations decrease sharply with increasing molecular weight (Figure 1b). These tendencies indicate that the internal unsaturations have the analytic characteristics of an "end group". That means, just as the number of end groups in a chain does not depend on its length, the number of internal unsaturations does not either. Monomer conversion did not change this tendency significantly (Figure 1). However, the total number of the defects increases with increasing conversion. This is consistent with our earlier study on nonfractionated polymers, where a steep increase in the number of internal unsaturations after monomer conversion of around 85% was observed.[12] Internal allylic functional groups are formed by hydrogen-transfer reactions of an inter- or intramolecular nature, *e.g.*, refs 1 and 5, and in a multiphase system (such as the suspension polymerization of VCM), the composition of the reaction phase is the most important factor determining the frequency of these side reactions. At 85% conversion, the polymerization proceeds exclusively in the polymer-rich phase, where the weight fraction of monomer is approximately 6% (calculated according to the model developed by Xie et al.[22]) and further decreases as the polymerization progresses (see Supporting Information for more details). The observed increase in the number of internal unsaturations with conversion can therefore be understood because the reduction of monomer concentration and concurrent increase in polymer concentration in the polymer-rich phase at conversions above 85%, favor hydrogen-transfer reactions.

It was proposed earlier[3] that the principal mechanism of formation of internal double bonds is an intermolecular transfer reaction—abstraction of H from the methylene unit by the growing macroradical (see Scheme 4, ref 12). Since this intermolecular transfer reaction can occur randomly along the chain, the concentration per 1000 VC should remain relatively constant, and the concentration per chain should increase sharply with increasing $\bar{M}_n$. Our current results indicate, in contrast, that only a small proportion (if any) of the internal unsaturations are likely to have been formed by intermolecular transfer reactions, while some even smaller proportion is probably formed by combination of allylic radicals.[12] However, since the concentration per 1000 VC drops dramatically with chain length, the overwhelming majority of the internal double bonds have to be formed via some other mechanism, after which the internal unsaturation behaves analytically as an end group.

Location of Internal Unsaturations. The above results thus suggest that the internal unsaturations behave analytically as an end group in VC polymerization. However, this does not necessarily mean that the internal unsaturation is physically the end group of the polymer. For example, as noted in the Introduction, one proposed mechanism for the formation of internal unsaturations involves hydrogen abstraction from chloroallylic end-groups. Such a mechanism would result in defect structures that function analytically as an "end group" but would result in the location of the internal unsaturations in the interior of the polymer chain. This differs from another proposed mechanism for the formation of internal unsaturated "end groups" in which internal double bonds are formed via an intramolecular 1−6 backbiting reaction followed by elimination of a Cl atom in the β position (see Scheme 1).[23] Also in this case, the internal double bond, once formed, stops further propagation of the polymer chain, and thus the internal unsaturation behaves analytically as an end group. However,

Scheme 3. Model Reactions Used in the Calculation of the Rate Coefficients for the Various Intramolecular Hydrogen Abstraction Reactions in Table 1

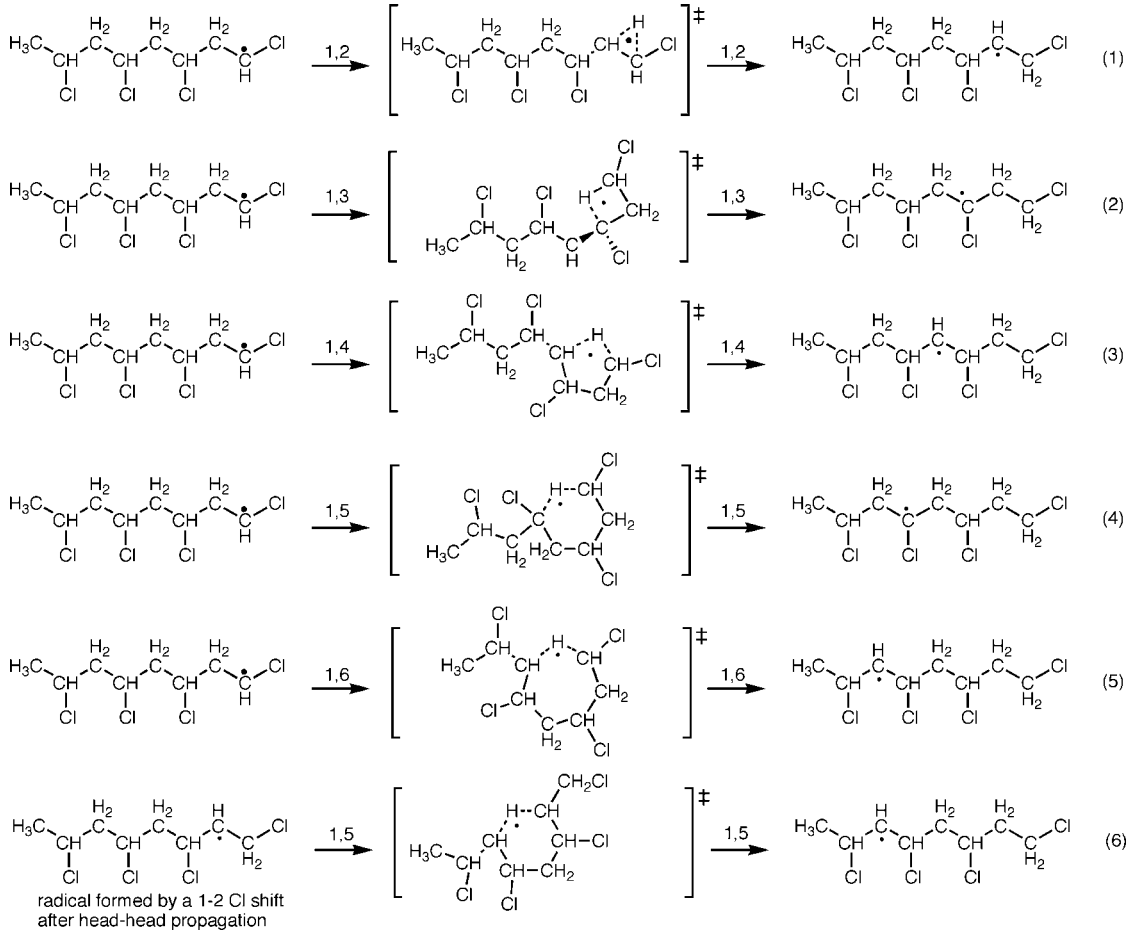

in contrast to the chloroallylic route, the reaction would always result in a double bond between carbons 5 and 6, or between carbons 6 and 7, depending upon which of the β-chlorine atoms is eliminated (see Scheme 1).

A method for discriminating between these alternative mechanisms for the formation of internal double bonds is the analysis of the ^{13}C spectra of reductively dehalogenated samples. Unsaturated structures undergo 1−5 free radical cyclizations upon reaction with Bu_3SnH, wherein a carbon-centered radical, formed from a C−Cl moiety, adds to a double bond to form a five-membered ring.[23] This addition results in various types of cyclopentane moieties, depending upon the location of the double bond in the chain (see also Scheme 2). The cyclic structures possess very similar chemical shifts,[23–26] but the monoalkylcyclopentane (MCP) structure that is formed by backbiting on a double bond in positions 5−6 (Scheme 2) can nevertheless be distinguished unambiguously in ^{13}C spectra. The chemical shifts of carbons α, 3 and 4 or 1 in the MCP structure (Scheme 2) have been determined (by comparison with ^{13}C spectra of model compounds)[23] not to overlap with those of other structures in reductively dehalogenated PVC. Figure 2 shows the ^{13}C spectrum of a low molecular weight, reductively dehalogenated PVC sample. MCP structures were most easily detectable in this fraction because of the larger content of unsaturations in the nonreduced sample. Even though the signals of MCP are very weak (probably due to nonquantitative cyclization), it is clear from the spectrum that the MCP structure is present. Hence, double bonds in the 5−6 position are present in our PVC. This accounts for the end-group-like behavior of the internal unsaturations. Although *n*-pentyl branches (products of a propagation of the 1−6 intramolecular rearranged radical) have not been found in ^{13}C spectra of PVC dehalogenated with Bu_3SnD,[28] Hjertberg et al.[3] have stated that only branches up to 5 carbons can be distinguished using ^{13}C spectra of reductively dehalogenated PVC.

At this point it should be noted that the evidence for formation of internal double bonds at the 5−6 position contrasts with earlier studies in which researchers found reductions in polymer molar mass after chain scission by ozone. In such an approach, the unsaturated structures resulting from 1−6 H transfer are not possible to measure because no detectable molecular weight reductions result from their ozonolytic removal, owing to their close proximity to the ends of polymer chains. Nevertheless Hjertberg and Sorvik[5,27] used ozonolysis to detect internal C=C contents of up to 0.78/1000 VC in a series of polymers made at 55 °C under subsaturation monomer pressures. Certainly our study does not rule out the presence of unsaturations located randomly in the polymer chain: the current NMR results do not exclude the presence of ICP structures that would result from their reductive cyclization, and, as noted above, this mechanism also results in internal unsaturations that function analytically as an end group, consistent with the observed molecular weight dependence of the defect structures. It is thus possible that multiple mechanisms are responsible for formation of internal unsaturations. However, the present work does indicate that formation of internal unsaturations between carbons 5−6 is a significant side reaction in the present polymerizations.

It should also be noted that internal unsaturations might be formed by other types of backbiting reactions. For example, a 1−4 backbiting reaction (Scheme 1) could also produce internal double bonds, which, upon reduction with Bu_3SnH, would give raise to butylcyclopentane moieties (Scheme 2). The ^{13}C signals

Scheme 4. Model Reactions Used To Calculate the Cl Transfer and β-H and β-Cl Elimination Reactions

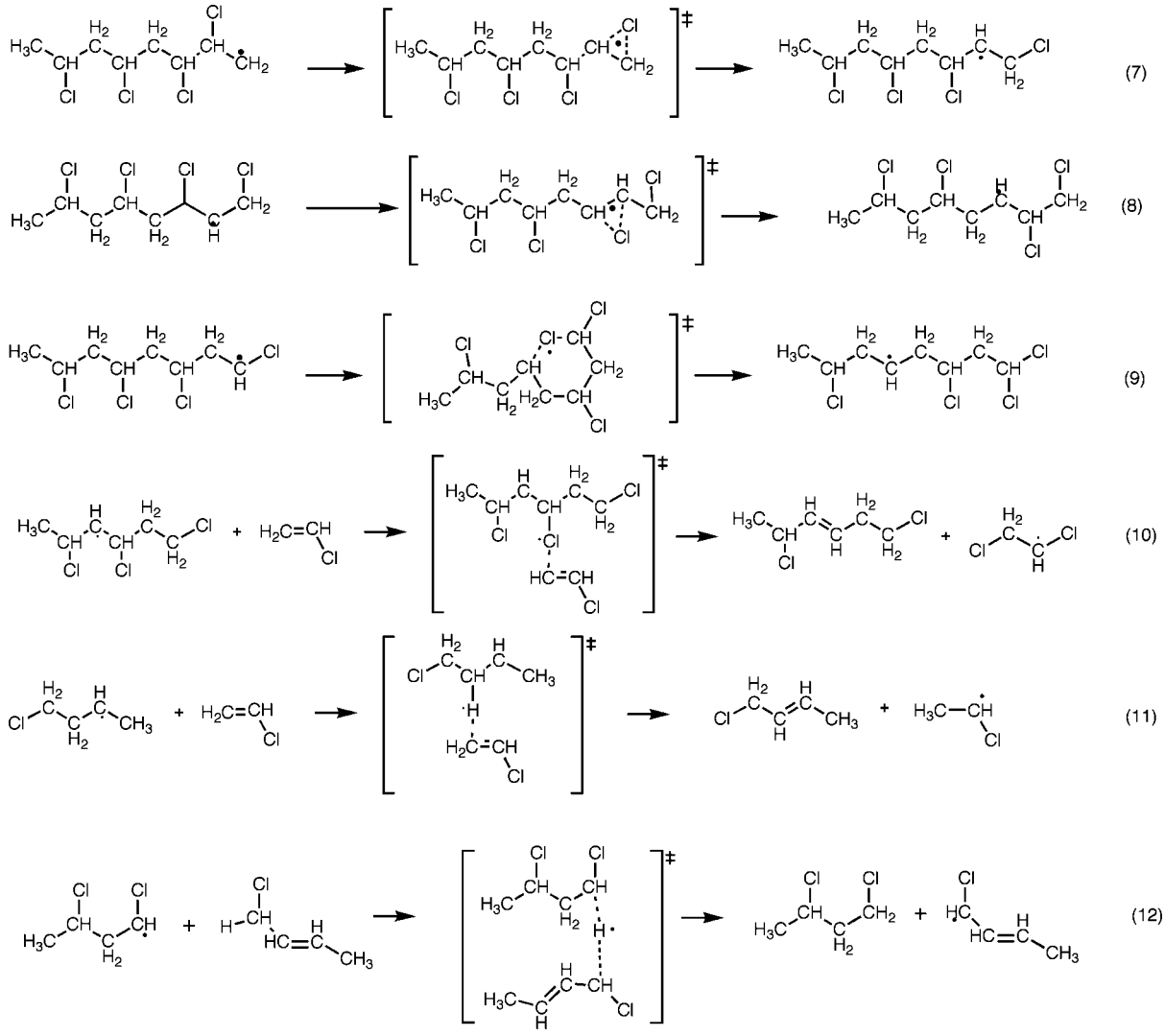

of such a structure are difficult to distinguish from the other cyclopentane moieties; however, it must be noted that propyl branches—which would result from the propagation of the intermediate radical—have never been detected in the ^{13}C NMR spectra of PVC[28] (although a possible reason might be that the intermediate radical undergoes β-chlorine scission before the propagation can take place).[23] In order to discriminate among the various possible mechanisms, the rate coefficient of the 1−4 transfer reactions was included in the ab initio molecular orbital calculations (see below). The rate coefficient of 1−5 backbiting was calculated as well in order to have a point of reference. This type of backbiting predominantly occurs in polymerization of many monomers such as ethylene,[29] acrylates,[30] and vinyl chloride. In the last case, the propagation of the intermediate radical is the origin of chlorobutyl branches, whose presence in PVC was previously reported.[3,28]

Before examining the ab initio calculations, it is worthwhile to note that backbiting appears to be stereoselective. It preferentially attacks the syndiotactic triads, while the isotactic conformation is more resistant. In Figure 3, the lower content of syndiotactic triads and higher content of isotactic triads in low molecular weight extracts of the 87.2 and 96.4% conversion polymers can be clearly seen. The higher content of isotactic triads in low molecular weight extracts is not an artifact of the isolation procedure,[31] as the same preference for isotactic triads was also seen in ether extracts and in some low molecular weight material obtained by fractionation. The differences in the sequence distribution of the low molecular weight part and complete PVC (samples of conversion above 87%) indicate that some portion of the syndiotactic triads is destroyed at the time when these short chains are formed. PVC with 23.7% conversion does not exhibit any difference in tacticity of low molecular weight part and nonfractionated polymer (Figure 3). It seems reasonable to suppose that the short chains of high conversion PVC are formed under conditions of monomer starvation where backbiting and subsequent Cl elimination (leading to the conversion of −CHCl− units to double bonds) are favored. It can be therefore assumed that the observed decrease in the number of syndiotactic triads is caused by intramolecular hydrogen abstraction. Short chains formed in the beginning of the polymerization (when plenty of monomer is available for propagation) undergo backbiting and Cl elimination less frequently, accounting for the lack of detectable differences in the content of iso- and syndiotactic triads.

The $-CH_2-$ group in a syndiotactic conformation probably provides less steric hindrance to backbiting from the radical chain end than the atoms in an isotactic conformation do. Indeed, ab initio molecular orbital calculations of the transition structures for the various types of backbiting reactions indicate that the Cl atoms tend to be orientated on alternating sides of the polymer chain in the lowest energy conformations (see Figure 4, and Figure 9 in ref 12).

Scheme 5. Model Reactions Used To Calculate the Propagation Reactions in Table 3

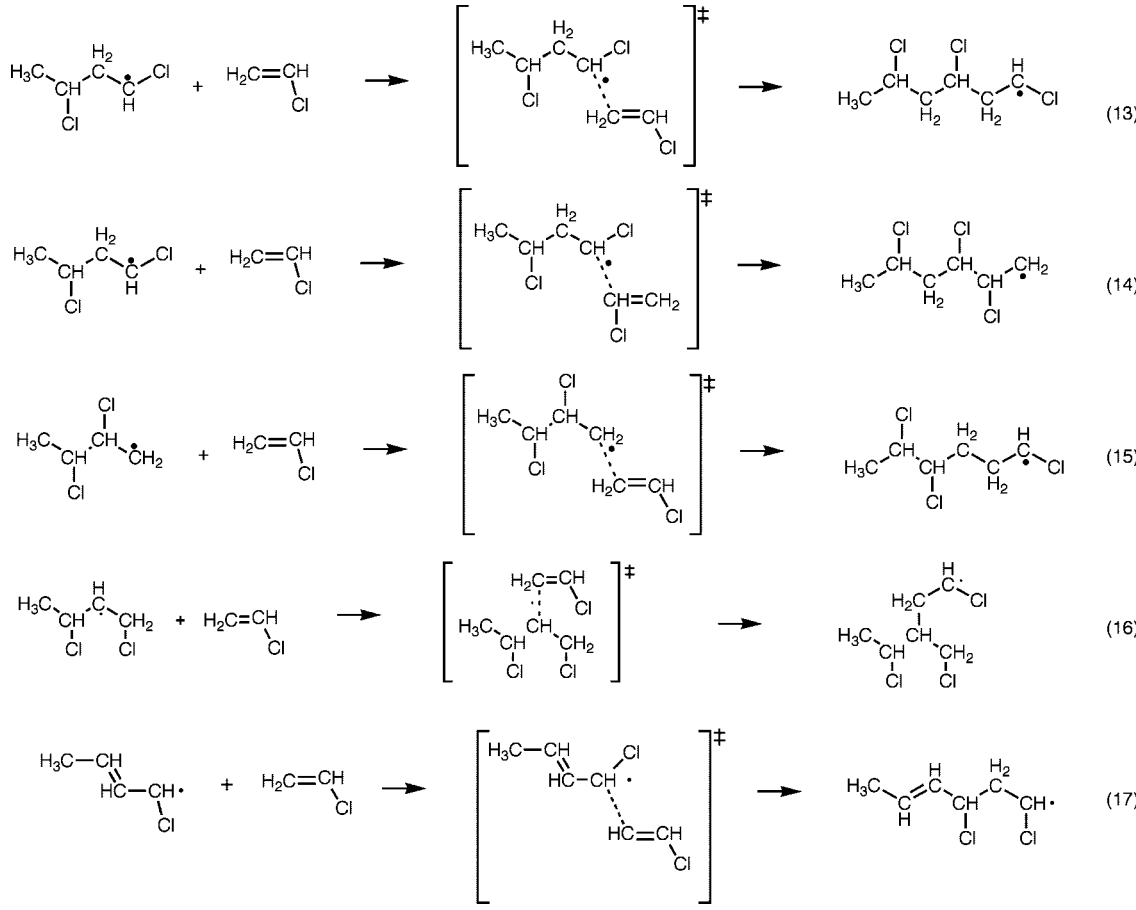

Scheme 6. Possible Defect Structures That Could Arise after a 1−5 Cl Shift

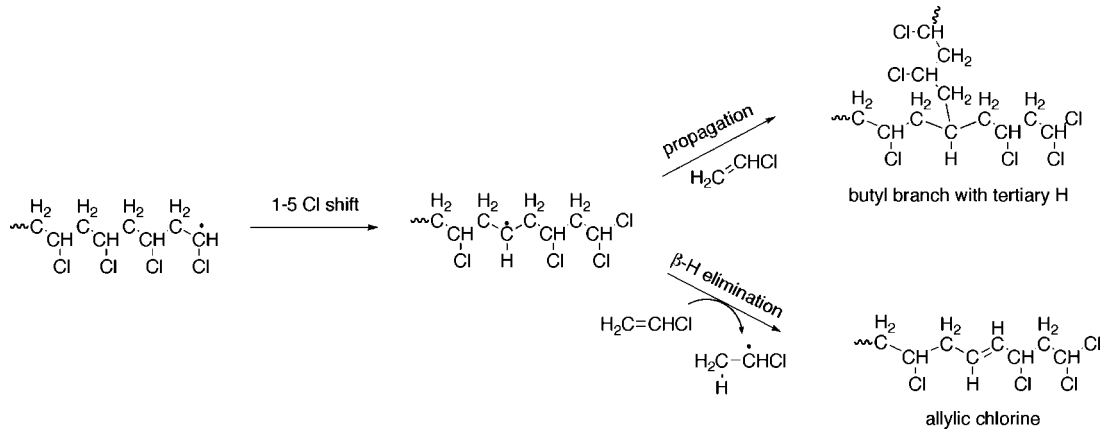

Theoretical Considerations. To help identify the origin of the internal unsaturations, rate coefficients (at 57.5 °C) for the model reactions depicted in Schemes 3 and 4 were calculated via ab initio molecular orbital theory and are shown in Tables 1 and 2, respectively. For the intramolecular hydrogen and chlorine atom transfer reactions, the propagating radical was modeled as a tetramer radical as this was necessary to accommodate some of the larger transition structures. For the majority of the other reactions, smaller (dimer) radicals were used as these were sufficient to accommodate the principal substituent effects on the reaction. We have shown previously that the rate coefficient for normal propagation converges to within a factor of 2 by the dimer stage.[21] There is also excellent agreement between the rate coefficient of the 1−2 hydrogen shift that we obtained previously[12] using a dimer propagating radical and that obtained in the present work for a tetramer species (see Table 1). The geometries of the transition structures are shown schematically in Figures 4, 5 and 7. Full geometries, in the form of GAUSSIAN archive entries, are provided in the Supporting Information.

Comparing first the rate coefficients for the intramolecular hydrogen abstractions of a normal propagating radical (reactions 1−6 in Table 1), the most favorable reaction is, as expected, the 1−5 shift. The 1−6 shift is the next most favorable, followed by the 1−4 shift. The 1−3 and 1−2 shifts, included in the Table for the sake of completeness, have negligible rate coefficients as expected. This trend reflects the fact that the 6-membered transition structure for the 1−5 shift has the least strained geometry, with strain increasing as the ring size departs from this optimal geometry. The entropies of activation actually favor

Table 1. Calculated Kinetic and Thermodynamic Parameters for the Intramolecular Hydrogen Transfer Reactions of the Vinyl Chloride Propagating Radical at 0 and 330.65 K[a]

reaction	1−2 (1)	1−2 (1′)[b]	1−3 (2)	1−4 (3)	1−5 (4)	1−6 (5)	1−5 H shift after a 1−2 Cl shift[c] (6)
$Q_{330.65}$	4.6×10^3	4.9×10^3	4.4×10^4	2.5×10^2	5.6×10^1	3.7×10^1	3.8×10^1
Forward Direction							
$\Delta H^{\ddagger}_0$ (kJ mol^{-1})	179.4	180.5	168.8	107.2	70.4	87.5	76.9
$\Delta H^{\ddagger}_{330.65}$ (kJ mol^{-1})	178.9	180.0	167.6	105.0	67.7	84.0	73.7
$\Delta S^{\ddagger}_{330.65}$ (J mol^{-1} K^{-1})	−4.1	−4.5	−3.3	−18.3	−33.2	−41.5	−36.8
$\Delta G^{\ddagger}_{330.65}$ (kJ mol^{-1})	180.3	181.5	168.7	111.0	78.7	97.8	85.8
$k_{330.65}$ (s^{-1})	1.0×10^{-12}	7.2×10^{-13}	6.9×10^{-10}	5.1×10^{-3}	1.4×10^2	9.2×10^{-2}	7.3
Reverse Direction							
$\Delta H^{\ddagger}_0$ (kJ mol^{-1})	175.2	176.9	172.8	103.4	68.8	84.1	78.0
$\Delta H^{\ddagger}_{330.65}$ (kJ mol^{-1})	174.2	175.8	194.3	100.6	66.4	80.1	74.9
$\Delta S^{\ddagger}_{330.65}$ (J mol^{-1} K^{-1})	−14.7	−13.3	177.0	−29.4	−42.1	−50.7	−35.4
$\Delta G^{\ddagger}_{330.65}$ (kJ mol^{-1})	179.0	180.2	135.8	110.3	80.3	96.8	86.6
$k_{330.65}$ (s^{-1})	1.7×10^{-12}	1.1×10^{-12}	1.1×10^{-4}	6.5×10^{-3}	8.0×10^1	1.3×10^{-1}	5.6

[a] Calculated at the G3(MP2)-RAD//MPW1K/6−31+G(d,p) level of theory. Rate coefficients (k) were calculated using simple transition state theory and incorporate Eckart tunneling corrections (Q) (see text). The Eckart tunneling corrections for reactions 1−6 were calculated using imaginary frequencies of 2039.8i, 2042.5i, 2244.3i, 1963.5i, 1878.9i, and 1765.7i cm^{-1}, respectively. The model reactions used for the calculations are shown in Scheme 3. [b] Dimer model used; taken from ref 12. [c] A 1−5 hydrogen transfer as per (4) but of the radical formed by the 1−2 Cl shift of a propagating radical formed via head-to-head addition.

Table 2. Calculated Kinetic Parameters for Chlorine Transfer and Elimination Reactions Potentially Associated with Defect Formation in PVC Polymerization at 330.65 K[a]

Reaction	1−2 Cl shift after HH propagation (7)	2nd 1−2 Cl shift after HH propagation followed by a 1−2 Cl shift (8)	1−5 Cl shift of normal propagating radical (9)	β-Cl elimination from midchain radical (10)	β-H elimination from midchain radical (11)	H abstraction from chloroallylic end group (12)
$Q_{330.65}$	1.0	1.0	1.7	1.0	9.96×10^2	17.2
Forward Direction						
$\Delta H^{\ddagger}_0$ (kJ mol^{-1})	37.0	35.7	153.5	39.8	89.1	32.9
$\Delta H^{\ddagger}_{330.65}$ (kJ mol^{-1})	35.5	34.6	150.9	42.4	89.1	33.3
$\Delta S^{\ddagger}_{330.65}$ (J mol^{-1} K^{-1})	−3.2	−10.3	−28.1	−116.0	−144.2	−144.1
$\Delta G^{\ddagger}_{330.65}$ (kJ mol^{-1})	36.6	38.0	160.3	80.7	136.8	81.0
$k_{330.65}$ (s^{-1} or L mol^{-1} s^{-1})	1.2×10^7	6.9×10^6	5.7×10^{-13}	3.3×10^1	4.5×10^{-5}	5.2×10^2
Reverse Direction						
$\Delta H^{\ddagger}_0$ (kJ mol^{-1})	41.2	31.0	125.4	25.0	110.6	93.2
$\Delta H^{\ddagger}_{330.65}$ (kJ mol^{-1})	39.4	30.2	122.5	27.4	111.5	94.7
$\Delta S^{\ddagger}_{330.65}$ (J mol^{-1} K^{-1})	−20.7	−9.6	−41.8	−127.0	−136.4	−133.2
$\Delta G^{\ddagger}_{330.65}$ (kJ mol^{-1})	46.3	33.3	136.3	69.4	156.6	138.8
$k_{330.65}$ (s^{-1} or L mol^{-1} s^{-1})	3.4×10^5	3.8×10^7	3.5×10^{-9}	2.1×10^3	3.4×10^{-8}	3.8×10^{-7}

[a] Calculated at the G3(MP2)-RAD//MPW1K/6−31+G(d,p) level of theory. Rate coefficients (k) were calculated using simple transition state theory and incorporate Eckart tunneling corrections (Q) (see text). The Eckart tunneling corrections for reactions (7)−(11) were calculated using imaginary frequencies of 135.3i, 122.9i, 780.4i, 166.9i, 2199.7i and 1804.4i cm^{-1}, respectively. The model reactions used for the calculations are shown in Scheme 4.

the smaller shifts (1−2 then 1−3 then 1−4) over the 1−5 shift, with the 1−6 being the least favorable. This is because there is a loss of vibrational entropy in the transition structure, which increases as a larger fraction of the reactant radical is constrained in a ring structure. Nonetheless, the differences in the barriers dominate the reactivity preferences such that the rate coefficient of the 1−5 shift of a normal propagating radical is approximately 1500 times faster than that of the 1−6 shift, 30000 times faster than that of the 1−4 shift, 11 orders of magnitude faster than the 1−3 shift and 14 orders of magnitude faster than the 1−2 shift.

Even though the 1−5 shift is the most favorable, this reaction is unlikely to give the unsaturated structures that we have detected. The formation of a 5−6 double bond from the 1−5 intermediate would require α-chlorine elimination, and the carbene involved in this process is a species of high energy whose formation would be enormously endothermic. Moreover, α-chlorine elimination from head-to-tail radicals would generate −CHClCH=CH_2 end groups, and, furthermore, the vinyl chloride/2-chloropropene copolymer would likewise contain a considerable amount of −CHClCH=$CHCH_3$ termini; these are situations that have previously been experimentally discounted.[32]

Nonzero slopes of the dependencies of the number of internal double bonds per chain on molecular weight (Figure 1a) might indicate that a small portion of internal unsaturations may be formed by an intermolecular chain transfer reaction. In our previous study we calculated the rate coefficient for intermolecular chain transfer to be 4.8 L mol^{-1} s^{-1}.[12] When the rates of both types of backbiting and intermolecular transfer (correcting the coefficients for the diffusion control, see Appendix II in the Supporting Information) are compared in form of $\log(\nu_{BB}/\nu_{tr\ inter})$ (Figure 6), it becomes obvious that even at high conversions intramolecular processes are much more favorable than intermolecular reactions.

In order to map completely all possible sources of internal double bonds, we have also considered several other mechanisms leading to double bonds at the position between carbon 5 and 6 or in the middle of the chain. One possibility is that the radical may undergo a 1−5 chlorine transfer, which, analogous to a 1−5 hydrogen transfer, produces an intermediate radical that can undergo two alternative fates. Its propagation would generate butyl branches with a hydrogen at the branch point carbon, while a β-hydrogen elimination would lead to unsaturation in the 5−6 position (see Scheme 6). Rate coefficients for these three steps are provided in Table 2 from which it will

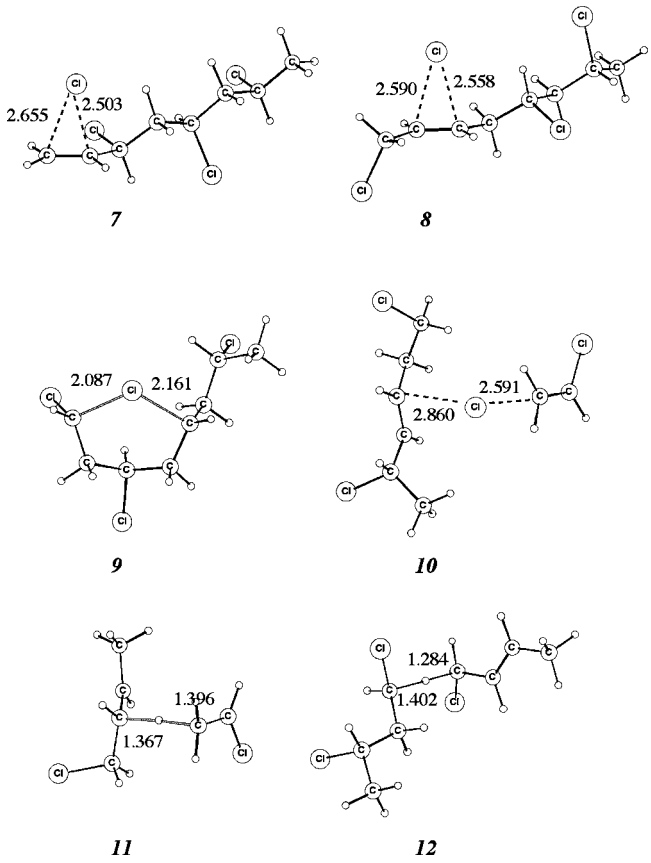

Figure 5. MPW1K/6−31+G(d,p) optimized geometries of the transition structures for the intramolecular chlorine transfer, β-Cl and H elimination reactions in Scheme 4.

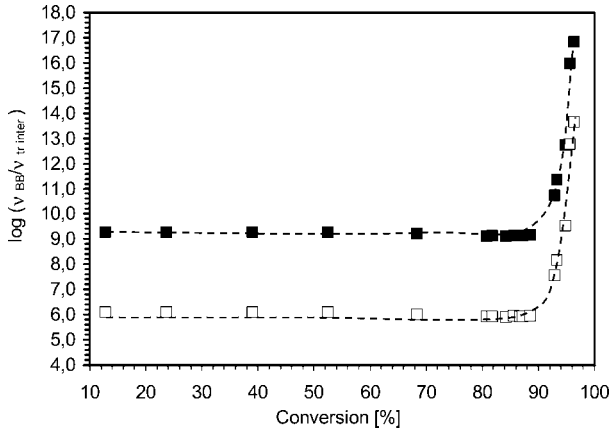

Figure 6. Correlation of the ratios of the rate of intermolecular transfer and 1−5 (□) and 1−6 (■) backbiting rates in the polymer-rich phase with monomer conversion during suspension VCM polymerization at 57.5 °C.

be seen that the rate coefficient for the initial 1−5 chlorine transfer (reaction 9 of Scheme 4) is so low (5.7×10^{-13} s^{-1}) that it could not out-compete the alternative hydrogen transfer reactions in Table 1. Moreover, even if this shift were to occur, the rate coefficient for the subsequent β-hydrogen elimination (reaction 10 of Scheme 4) is approximately 8 orders of magnitude lower than that of the competing propagation step (reaction 14 of Scheme 5) and the reaction would thus yield branches rather than internal unsaturations.

Another possible route to 5−6 unsaturations is a three-step pathway in which the propagating radical undergoes head-to-head addition with vinyl chloride monomer, followed by a 1−2 chlorine shift and then a 1−5 hydrogen transfer (see Scheme 7). The product radical of this process would then be identical to that of a direct 1−6 hydrogen transfer and be able to undergo β-Cl elimination in the usual manner. The first two reactions in this sequence are well-known in PVC chemistry and the third seems plausible given the high frequency of 1−5 hydrogen transfer reactions for normal propagating radicals. From Table 2, we note that the rate coefficient for head-to-head addition (reaction 14 of Scheme 5) is only 25 times lower than that for normal propagation (reaction 13 of Scheme 5) and would thus be a significant side-reaction, as expected. Moreover, the rate coefficient for the 1−2 Cl shift (reaction 7 of Scheme 4) is sufficiently high that, even at high monomer concentrations, this shift would normally follow head-to-head addition. The rate coefficient for the subsequent 1−5 hydrogen shift of this radical (reaction 6 of Scheme 3) is slightly smaller than that of a normal 1−5 hydrogen shift (reaction 4 of Scheme 3), which probably reflects the greater steric hindrance at the radical center. Nonetheless the rate coefficient is considerably larger than that of a 1−6 hydrogen shift (reaction 5 of Scheme 3) and such a reaction could plausibly be involved in the formation of internal unsaturations. At a monomer concentration of 1 mol L^{-1}, the rate of the unimolecular 1−5 hydrogen transfer reaction of the 1−2 Cl-shifted radical is approximately 330 times smaller than that of the competing bimolecular propagation (reaction 13 in Scheme 5). Thus, at low conversion, the propagation reaction is expected to dominate; however at high conversion (conditions of monomer starvation), it is possible that the 1−5 hydrogen transfer could out-compete propagation, leading to the internal unsaturations. This is examined more quantitatively below with consideration of the appropriate corrections for diffusion control. It is worthwhile to note that the radical formed by a second chlorine shift (reaction 8 in Scheme 4) might undergo 1−5 backbiting too. However, the formation of internal unsaturations from the resulting tertiary chlorine-containing radical is unlikely from the same reasons as in the case of 1−5 backbiting of the head-to-tail radical (see earlier in the text).

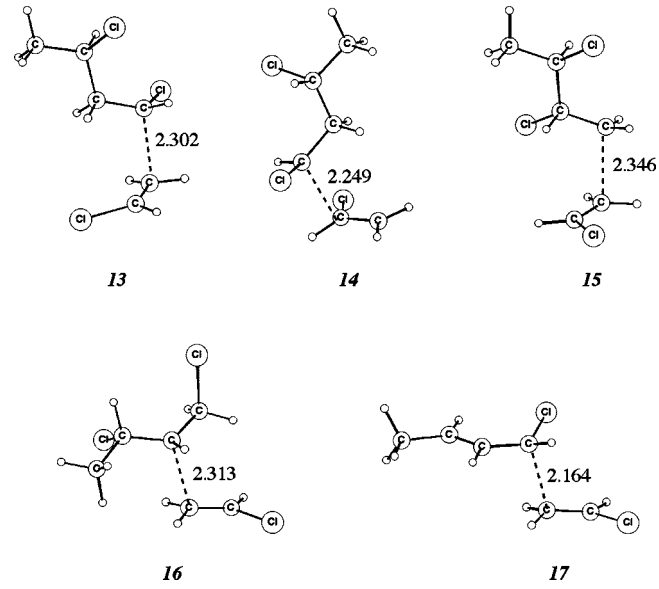

Figure 7. MPW1K/6−31+G(d,p) optimized geometries of the propagation reactions in Scheme 5.

Finally, the rate coefficients of hydrogen abstraction from a chloroallylic end group and of propagation of the resulting radical were calculated (Table 2 and 3). As explained above, this reaction is the most likely candidate to generate unsaturations in the middle of the polymer chain but behaving analytically as an end group.

Scheme 7. Possible Reactions Involving the Head-to-Head Radical in Vinyl Chloride Polymerization

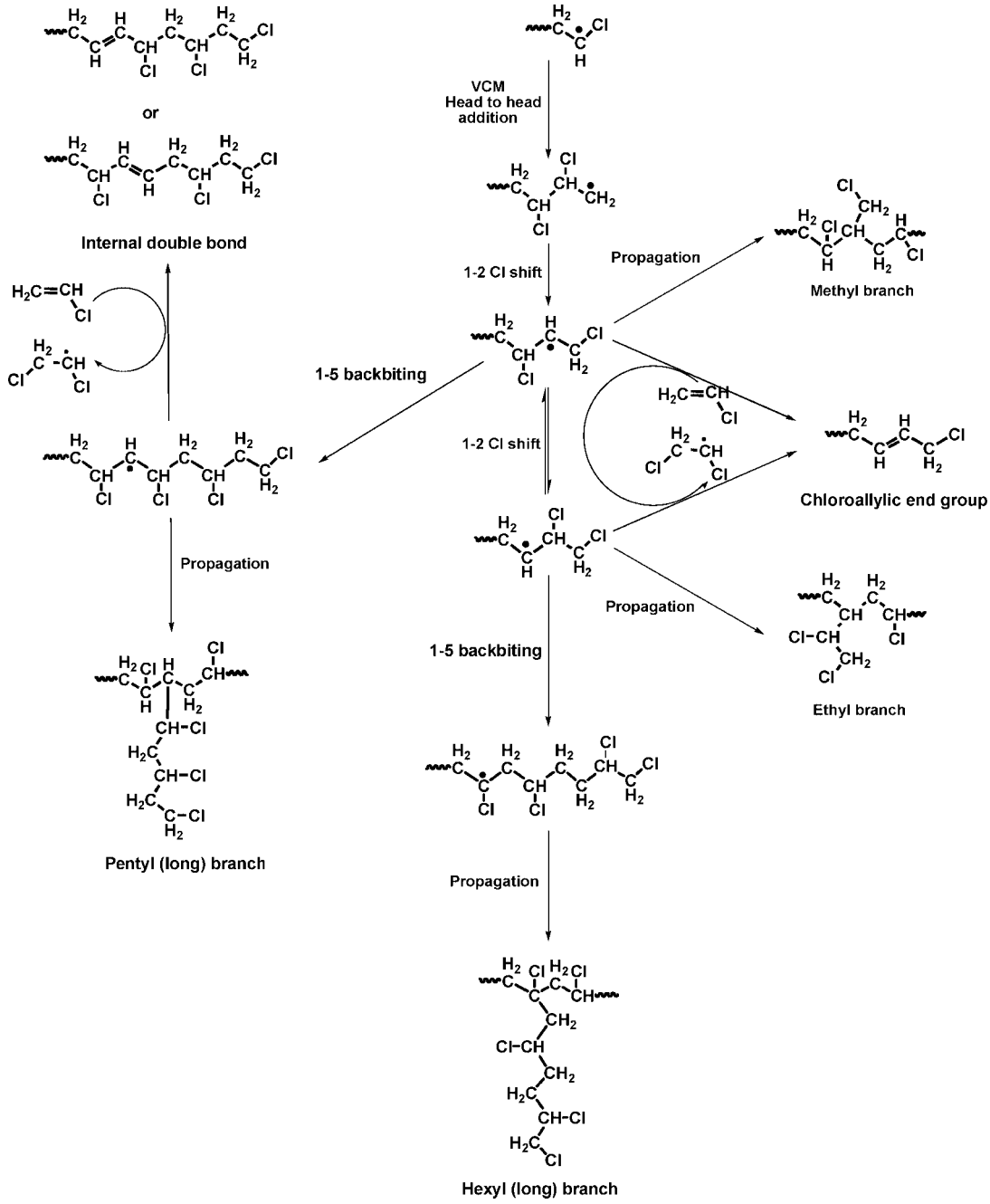

Table 3. Calculated Kinetic Parameters for Potential Propagation Reactions in PVC at 0 and 330.65 K[a]

reaction	normal propagation (13)[b]	head-to-head (HH) propagation (14)	normal propagation by head-to-head adduct (15)	propagation of midchain radical (16)	propagation of allylic radical (17)
$\Delta H^{\ddagger}_0$ (kJ mol^{-1})	12.6	18.4	16.5	14.7	44.6
$\Delta H^{\ddagger}_{330.65}$ (kJ mol^{-1})	11.6	17.2	15.2	13.2	43.6
$\Delta S^{\ddagger}_{330.65}$ (J mol^{-1} K^{-1})	−159.4	−169.1	−156.3	−168.7	−159.8
$\Delta G^{\ddagger}_{330.65}$ (kJ mol^{-1})	64.3	73.1	66.9	68.9	96.4
$k_{330.65}$ (L mol^{-1} s^{-1})	1.3×10^4	5.3×10^2	5.1×10^3	2.4×10^3	1.1×10^{-1}

[a] Calculated at the G3(MP2)-RAD//MPW1K/6-31+G(d,p) level of theory. Rate coefficients (k) were calculated using simple transition state theory. The model reactions used for the calculations are shown in Scheme 5 [b] Taken from ref 12.

Comparison of the Proposed Intramolecular Mechanisms Leading to Internal Unsaturations. A three-step pathway involving head-to-head addition, 1−2 chlorine migration, and 1−5 (with respect to the radical center) hydrogen abstraction (Scheme 7), 1–6 intramolecular hydrogen transfer (Scheme 1), intermolecular hydrogen abstraction and propagation of chloroallyl radical (reaction 17 in Scheme 5) all seem to be plausible mechanisms to explain the end-group-like characteristics of internal unsaturations in PVC. To compare these mechanisms quantitatively, we have calculated—with the help of formulas 32−54 in Supporting Information—the probabilities of each of these pathways. Calculation of the monomer and polymer concentrations necessary to obtain the reaction rates can be also found there. Rate coefficients necessary to calculate the prob-

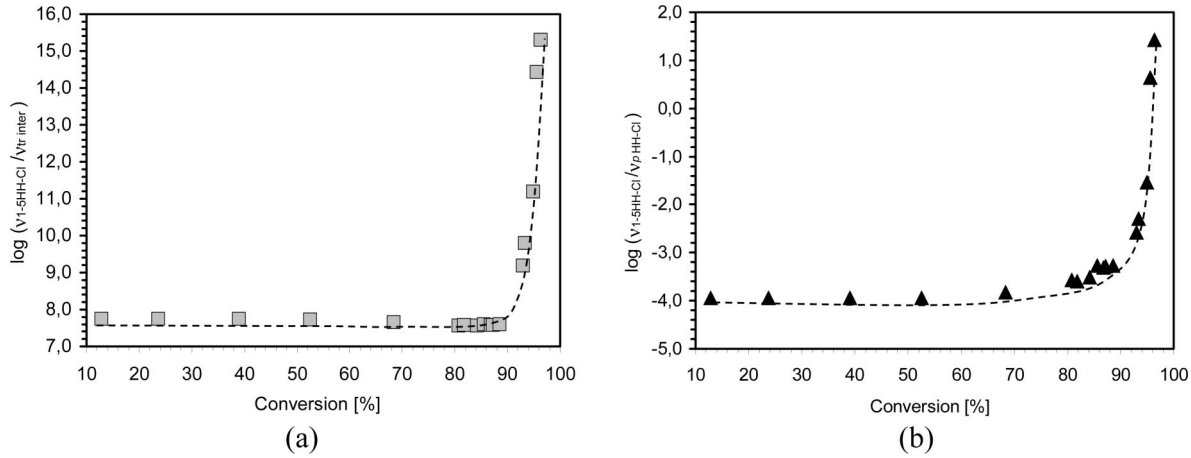

Figure 8. Monomer conversion dependence of the ratio between the rate of 1−5 backbiting of the rearranged head-to-head radical and (a) intermolecular hydrogen transfer or (b) propagation of the same radical.

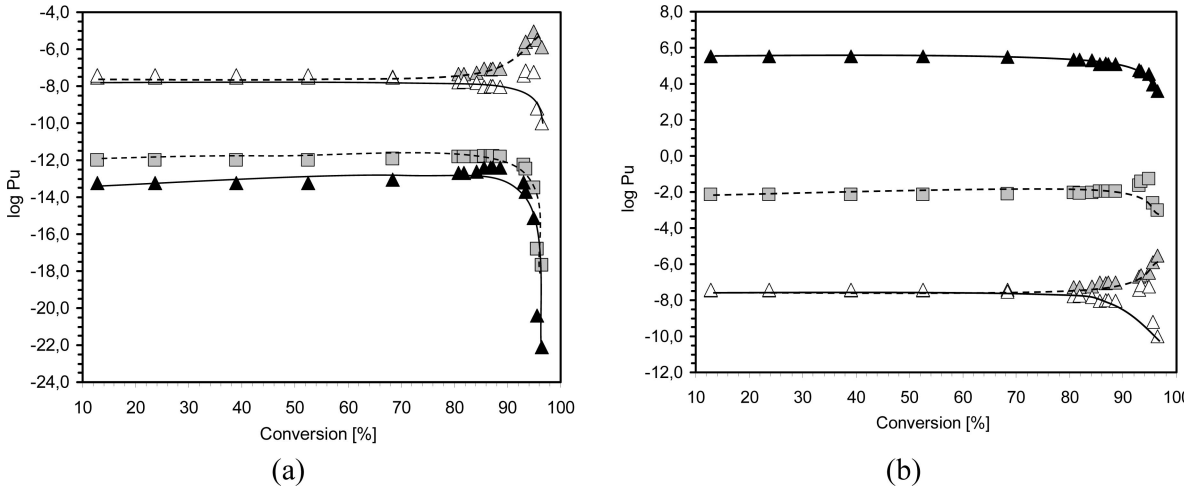

Figure 9. Relationship between monomer conversion and the probabilities of the formation of internal unsaturations (P_u) by (grey triangle) 1−6 backbiting, (▲) intermolecular hydrogen abstraction, (grey square) hydrogen abstraction of chloroallylic end group, and (△) 1−5 backbiting of a 1−2 chlorine shifted head-to-head radical. Probabilities were calculated (a) with and (b) without correction for diffusion control.

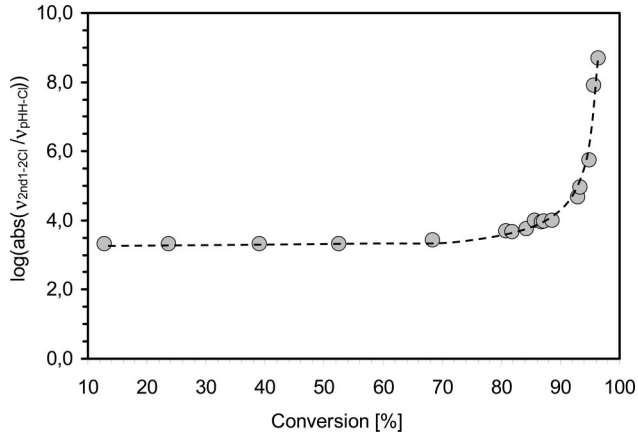

Figure 10. Monomer conversion dependence of the ratio between the rate of second chlorine shift after head-to-head addition and propagation of the 1−2 Cl shifted head-to-head radical.

abilities were obtained by high level ab initio calculations and can be found in Tables 1, 2, and 3. Where relevant, the rate coefficients were corrected for diffusion control; these corrections are described in full in the Supporting Information.

Figure 8a compares the rates of the three step 1−5 hydrogen transfer process ($\nu_{1-5\text{-HHCl}}$) with the direct intermolecular hydrogen abstraction route ($\nu_{\text{tr inter}}$). The rate of the 1−5 hydrogen transfer process is much higher than that for intermolecular hydrogen transfer from dead polymer chains as can be seen from the development of the $\log(\nu_{1-5\text{-HHCl}}/\nu_{\text{tr inter}})$ with conversion.

Figure 8b compares the rates of the 1−5 hydrogen transfer process with the competing propagation step of the same midchain radical (ν_{pHHCl}) as a function of conversion. At conversions below approximately 90%, the transfer is lower than the rate of propagation of the same radical; however, beyond 90% conversion, the monomer concentration drops and the transfer reaction becomes a significant side reaction.

Figure 9 compares the overall probability of the three step 1−5 hydrogen transfer process with that of hydrogen abstraction of chloroallylic end group, intermolecular hydrogen abstraction and the direct 1−6 transfer route. When diffusion control is taken into account, the probability that internal double bonds will be formed by intermolecular hydrogen transfer is the lowest; the probability that they form via hydrogen abstraction from a chloroallylic end group is marginally higher; the various intramolecular pathways are the most favorable. Of these latter mechanisms, the three step mechanism and 1−6 backbiting display about the same probability until around 90% of monomer conversion. Then the probability of 1−6 backbiting increases while the possibility of three step mechanism becomes lower. The crucial condition for the three step mechanism is the head-to-head monomer addition and for the allyl route it is the

propagation. In particular, beyond 90% conversion, further decreases in the monomer concentration allow the 1−6 shift to compete effectively with the mechanisms requiring addition of monomer.

It should, however, be noted that, if the effects of diffusion are ignored, a totally different picture is obtained. In that case, intermolecular transfer is the most favorable followed by H abstraction from chloroallylic end groups, with both intramolecular routes being less favorable than intermolecular counterparts. It is thus clear that the effects of diffusion, which reduces the rates of intermolecular reactions relative to the intramolecular ones, play an important role in determining the mechanistic outcome. It is therefore possible that, if the effects of diffusion have been overestimated using the model of De Roo et al.,[33] the pathway involving hydrogen abstraction from chloroallylic end groups could become competitive with the intramolecular pathways, resulting in internal unsaturations in interior of the polymer chain, in addition to those formed at carbons 5−6. As noted above, both pathways are consistent with the observed molecular weight dependence of the internal defect structures, and while the NMR studies provide clear evidence for defect structures between carbons 5 and 6, this evidence was not quantitative. The concurrent involvement of both the intramolecular and chloroallylic end group pathways would be a means of reconciling the seemingly conflicting evidence from the present work and the earlier ozonolytic analysis performed by Hjertberg and Sorvik.[5,27]

Relation to the Number of Defects Structures in Nonfractionated PVC. Propagation of a radical resulting from 1−6 hydrogen transfer (and also of the one formed by the above-described three-step mechanism) would render an *n*-pentyl branch carrying hydrogen on its branch point carbon. This structure would be detected as a long-chain branch in the ^{13}C NMR spectra of reductively dehalogenated PVC.[3] As can be seen from Scheme 6, a 1−2 Cl shifted head-to-head radical can undergo four possible reactions: propagation (renders methyl branches), β-Cl elimination (chloroallylic end groups), Cl shift and 1−5 backbiting with its subsequent reactions (internal double bonds and long-chain branches). β-Cl elimination seems to be the least favorable reaction, because the number of chloroallylic end groups is only about 0.7 per 1000 VC in nonfractionated PVC. On the basis of the number of defects (∼5 per 1000 VC), propagation leading to methyl branches looks to be the most favorable. The reverse rate coefficient of the second Cl shift is higher than forward rate coefficient of this reaction (Table 2). Considering propagation an irreversible reaction, propagation of the 1,2 Cl shifted HH (midchain) radical is more favorable than second Cl shift. The ratio of the rates of these reactions will be therefore always negative. Figure 10 shows the log of the absolute value of this ratio plotted against conversion. This figure can be interpreted in the terms of second Cl shift becoming more favorable at high conversions, where low monomer concentration slows down the propagation. This is confirmed by the number of ethyl branches—defects arising from propagation of radical after second Cl shift—and their tendency to increase with conversion (0.4 per 1000 VC units).

Conclusions and Implications

The present study challenges the notion that internal unsaturated bonds in PVC arise from intermolecular hydrogen abstractions from the middle of the polymer chain. It was found that the concentration of these groups per chain increased only slightly with molecular weight, and that the concentration per 1000 VC decreased dramatically which indicates that the group behaves analytically as an end group. The presence of unsaturation between carbons 5 and 6 was confirmed via ^{13}C NMR studies of reductively dehalogenated polymers, and high-level ab initio calculations showed that a 1−6 backbiting hydrogen transfer reaction is a plausible origin for these structures, consistent with the earlier proposal of Starnes et al.[23] The backbiting reaction seems to be stereoselective, with the isotactic conformation appearing to be more resistant. However, on taking into account all of the theoretical and experimental evidence from the present work and earlier studies, it seems likely that hydrogen abstraction from chloroallylic end groups and further propagation of such radical is a concurrent route to internal double bonds.

Efforts to improve the thermostability of PVC should thus be directed at minimizing hydrogen abstraction reactions, especially backbiting and hydrogen abstraction from chloroallylic end groups. One option, currently being explored in our laboratory, is to restrict the mobility of the polymer chains by creating a denser polymer-rich phase by addition of a precipitant for PVC. Another possible approach is the reversible complexation of the radical chain end with a compound containing a functional group that is able to interact with the PVC molecule. Promising results have been obtained when compounds containing cyclic ester groups were added to the polymerization mixture. Both of these approaches will be the subject of our next publications.

Acknowledgment. We would like to thank to Dutch Ministry of Economical Affairs (SENTER-IOP) for financial support and the members of the IOP steering committee for helpful discussions. M.L.C gratefully acknowledges computational assistance from Dr. Elizabeth Krenske, generous allocations of computing time from the Australian Partnership for Advanced Computing and financial support from the Australian Research Council.

Supporting Information Available: Table S1, showing the characteristics of the PVC samples, Table S2, showing the MPW1K/6−31+G(d,p) optimized geometries of the reactants, products, and transition structures, in the form of GAUSSIAN archive entries, Figure S1, showing the development of the monomer fraction in the polymer-rich phase with the course of the polymerization, and appendices with text giving, finally, a detailed description of the calculation of the number of structural defects, determination of the polymer-rich phase composition and calculation of the diffusion controlled rate coefficients and probabilities of different side reactions. This material is available free of charge via the Internet at http://pubs.acs.org.

References and Notes

(1) Starnes, W. H., Jr. *Prog. Polym. Sci.* **2002**, *27*, 2133–2170.
(2) (a) Asahina, M.; Onozuka, M. *J. Polym. Sci., Part A: Polym. Chem.* **1964**, *2*, 3505–3513. (b) Asahina, M.; Onozuka, M. *J. Polym. Sci., Part A: Polym. Chem.* **1964**, *2*, 3515–3522.
(3) Hjertberg, T.; Sörvik, E. M. *Polymer* **1983**, *24*, 673–684.
(4) Darricades-Llauro, M. F.; Michel, A.; Guyot, A.; Waton, R.; Pétiaud, R.; Pham, Q. T. *J. Macromol. Sci., Chem.* **1986**, *A23*, 221–269.
(5) Hjertberg, T.; Sörvik, E. M. *Polymer* **1983**, *24*, 685–692.
(6) Reviewed in, e.g. :(a) Minsker, K. S. *J. Vinyl Technol.* **2001**, *7*, 222–234. (b) Endo, K. *Prog. Polym. Sci.* **2002**, *27*, 2021–2054.
(7) Reviewed in: Steenwijk, J. (Natural) Polyols as stabilisers for heavy metal-free PVC: the stabilising mechanism and the influence on rheology. *Dissertation*, Utrecht University, **2003**; pp 15−27.
(8) http://www.stabilisers.org/pr2003/PROGRESS%20REPORT%202003.pdf, **2003**, 13−14.
(9) Starnes, W. H., Jr.; Girois, S. *Polym. Yearbook* **1995**, *12*, 105–131.
(10) Starnes, W. H., Jr.; Chung, H.; Wojciechowski, B. J.; Skillicorn, D. E.; Benedikt, G. M. *Adv. Chem. Ser.* **1996**, *249*, 3–18.
(11) Xu, P.; Zhou, D.; Zhao, D. *Eur. Polym. J.* **1989**, *25*, 581–583.
(12) Purmová, J.; Pauwels, K. F. D.; Van Zoelen, W.; Vorenkamp, E. J.; Schouten, A. J.; Coote, M. L. *Macromolecules* **2005**, *38*, 6352–6366.
(13) Kotera, A. In: *Polymer Fractionation*; Cantow, M. J. R. Ed.; Academic Press: New York, London, 1967; pp 44−65.
(14) Purmová, J.; Pauwels, K. F. D.; Agostini, M.; Bruinsma, M.; Schouwstra, J. R.; Vorenkamp E. J.; Schouten, A. J.; Coote, M. L. Submitted for publication.

(15) Hjertberg, T.; Wendel, A. *Polymer* **1982**, *23*, 1641–1645.
(16) Starnes, W. H., Jr.; Hartless, R. I.; Schilling, F. C.; Bovey, F. A. *Polym.Prepr.* **1977**, *18*, 499–504.
(17) Frisch, M. J.; Trucks, G. W.; Schlegel, H. B.; Scuseria, G. E.; Robb, M. A.; Cheeseman, J. R.; Montgomery, J. A., Jr. ; Vreven, T.; Kudin, K. N.; Burant, J. C.; Millam, J. M.; Iyengar, S. S.; Tomasi, J.; Barone, V.; Mennucci, B.; Cossi, M.; Scalmani, G.; Rega, N.; Petersson, G. A.; Nakatsuji, H.; Hada, M.; Ehara, M.; Toyota, K.; Fukuda, R.; Hasegawa, J.; Ishida, M.; Nakajima, T.; Honda, Y.; Kitao, O.; Nakai, H.; Klene, M.; Li, X.; Knox, J. E.; Hratchian, H. P.; Cross, J. B.; Adamo, C.; Jaramillo, J.; Gomperts, R.; Stratmann, R. E.; Yazyev, O.; Austin, A. J.; Cammi, R.; Pomelli, C.; Ochterski, J. W.; Ayala, P. Y.; Morokuma, K.; Voth, G. A.; Salvador, P.; Dannenberg, J. J.; Zakrzewski, V. G.; Dapprich, S.; Daniels, A. D.; Strain, M. C.; Farkas, O.; Malick, D. K.; Rabuck, A. D.; Raghavachari, K.; Foresman, J. B.; Ortiz, J. V.; Cui, Q.; Baboul, A. G.; Clifford, S.; Cioslowski, J.; Stefanov, B. B.; Liu, G.; Liashenko, A.; Piskorz, P.; Komaromi, I.; Martin, R. L.; Fox, D. J.; Keith, T.; Al-Laham, M. A.; Peng, C. Y.; Nanayakkara, A.; Challacombe, M.; Gill, P. M. W.; Johnson, B.; Chen, W.; Wong, M. W.; Gonzalez, C.; Pople, J. A. *Gaussian 03, Revision B.03*; Gaussian, Inc.: Pittsburgh PA, 2003.
(18) Werner, H.-J.; Knowles, P. J.; Amos, R. D.; Bernhardsson, A.; Berning, A.; Celani, P.; Cooper, D. L.; Deegan, M. J. O.; Dobbyn, A. J.; Eckert, F.; Hampel, C.; Hetzer, G.; Korona, T.; Lindh, R.; Lloyd, A. W.; McNicholas, S. J.; Manby, F. R.; Meyer, W.; Mura, M. E.; Nicklass, A.; Palmieri, P.; Pitzer, R.; Rauhut, G.; Schütz, M.; Stoll, H.; Stone, A. J.; Tarroni, R.; Thorsteinsson, T. *MOLPRO 2000.6*; University of Birmingham: Birmingham, U.K., 1999.
(19) Coote, M. L. *J. Phys. Chem. A* **2004**, *108*, 3865–3872.
(20) Coote, M. L.; Collins, M. A.; Radom, L. *Mol. Phys.* **2003**, *101*, 1329–1338.
(21) Izgorodina, E. I.; Coote, M. L. *Chem. Phys.* **2006**, *324*, 96–110.
(22) Xie, T. Y.; Hamielec, A. E.; Wood, P. E.; Woods, D. R. J. *Appl. Polym. Sci.* **1987**, *34*, 1749–1766.
(23) Starnes, W. H., Jr.; Zaikov, V. G.; Chung, H. T.; Wojciechowski, B. J.; Tran, H. V.; Saylor, K.; Benedikt, G. M. *Macromolecules* **1998**, *31*, 1508–1517.
(24) Starnes, W. H., Jr.; Villacorta, G. M.; Schilling, F. C.; Park, G. S.; Saremi, A. H. *Polym.Prepr.* **1983**, *24*, 253–254.
(25) Starnes, W. H., Jr.; Villacorta, G. M.; Schilling, F. C. *Polym. Prepr.* **1981**, *22*, 307–308.
(26) Galimberti, M.; Albizzati, E.; Abis, L.; Bacchilega, G. *Makromol. Chem.* **1991**, *192*, 2591–2601.
(27) Hjertberg, T.; Sörvik, E. M. *ACS Symp. Ser.* **1985**, *280*, 259–284.
(28) Starnes, W.H., Jr.; Schilling, F. C.; Plitz, I. M.; Cais, R. E.; Freed, D. J.; Hartless, R. I.; Bovey, F. A. *Macromolecules* **1983**, *16*, 790–807, and references cited therein.
(29) See, e.g.: (a) Roedel, M. J. *J. Am. Chem. Soc.* **1953**, *75*, 6110–6133. (b) Boundy, R. H.; Boyer, R. F. *Styrene-Its Polymers, Copolymers and Derivatives*; ACS Monograph Series 115;Reinhold Publ. Con: New York, 1952; p 231. (c) Usami, T.; Takayama, S. *Macromolecules* **1984**, *17*, 1756.
(30) See e.g.: (a) Yamada, B.; Azukizawa, M.; Yamazoe, H.; Hill, D.; Pomery, P. J. *Polymer* **2000**, *41*, 5611–5618. (b) Farcet, C.; Belleney, J.; Charleux, B.; Pirri, R. *Macromolecules* **2002**, *35*, 4912.
(31) Martínez, G.; Mijangos, C.; Millán, J.; Alemany, A. *Makromol.Chem.* **1986**, *187*, 2649–2653.
(32) Braun, D.; Weiss, F. *Angew. Makromol. Chem.* **1970**, *13*, 55–66.
(33) De Roo, T.; Heynderickx, G. J.; Marin, G. B. *Macromol. Symp.* **2004**, *206*, 215–228.

MA800583K